



Since January 2020 Elsevier has created a COVID-19 resource centre with free information in English and Mandarin on the novel coronavirus COVID-19. The COVID-19 resource centre is hosted on Elsevier Connect, the company's public news and information website.

Elsevier hereby grants permission to make all its COVID-19-related research that is available on the COVID-19 resource centre - including this research content - immediately available in PubMed Central and other publicly funded repositories, such as the WHO COVID database with rights for unrestricted research re-use and analyses in any form or by any means with acknowledgement of the original source. These permissions are granted for free by Elsevier for as long as the COVID-19 resource centre remains active.



# Venezuelan equine encephalitis virus non-structural protein 3 (nsP3) interacts with RNA helicases DDX1 and DDX3 in infected cells



Moushimi Amaya<sup>a</sup>, Taryn Brooks-Faulconer<sup>a</sup>, Tyler Lark<sup>a</sup>, Forrest Keck<sup>a</sup>, Charles Bailey<sup>a</sup>, Venu Raman<sup>b</sup>, Aarthi Narayanan<sup>a,\*</sup>

<sup>a</sup> National Center for Biodefense and Infectious Diseases, George Mason University, Manassas, VA, United States

<sup>b</sup> Johns Hopkins University, Departments of Radiology and Oncology, Maryland, United States

## ARTICLE INFO

### Article history:

Received 8 March 2016

Received in revised form

12 April 2016

Accepted 13 April 2016

Available online 20 April 2016

## ABSTRACT

The mosquito-borne New World alphavirus, Venezuelan equine encephalitis virus (VEEV) is a Category B select agent with no approved vaccines or therapies to treat infected humans. Therefore it is imperative to identify novel targets that can be targeted for effective therapeutic intervention. We aimed to identify and validate interactions of VEEV nonstructural protein 3 (nsP3) with host proteins and determine the consequences of these interactions to viral multiplication. We used a HA tagged nsP3 infectious clone (rTC-83-nsP3-HA) to identify and validate two RNA helicases: DDX1 and DDX3 that interacted with VEEV-nsP3. In addition, DDX1 and DDX3 knockdown resulted in a decrease in infectious viral titers. Furthermore, we propose a functional model where the nsP3:DDX3 complex interacts with the host translational machinery and is essential in the viral life cycle. This study will lead to future investigations in understanding the importance of VEEV-nsP3 to viral multiplication and apply the information for the discovery of novel host targets as therapeutic options.

© 2016 Elsevier B.V. All rights reserved.

## 1. Introduction

The DEAD-box RNA helicases play multi-functional roles in RNA transcription, pre-mRNA splicing, ribosome biogenesis, RNA transport, translation initiation and RNA decay (Edgcomb et al., 2012; Fuller-Pace, 2013; Ishaq et al., 2009; Valiente-Echeverria et al., 2015; Xu et al., 2010). Recently evidence in the literature suggests that interactions with RNA helicases contribute to the lifecycle of positive sense RNA viruses. For example, DDX1 facilitates replication of a number of viruses such as: Human immunodeficiency virus 1 (HIV-1) by interacting with HIV-1 Rev protein (Edgcomb et al., 2012); severe acute respiratory syndrome coronavirus, infectious bronchitis virus and mouse hepatitis virus (MHV) JHM strain (JHMV) through interactions with nsp14 (Xu et al., 2010) and phosphorylated nucleocapsid protein (Wu et al., 2014); and Hepatitis C virus (HCV) by binding to the 3'(+)-UTR and 5'(-) UTR (Tingting et al., 2006). Besides DDX1, DDX3, facilitates replication of Japanese encephalitis virus (JEV) through

interactions with JEV NS3 and NS5 proteins, and the 5' and 3' UTR (Li et al., 2014); HIV-1 by interactions with HIV-1 Tat (Lai et al., 2013; Yasuda-Inoue et al., 2013) and HIV-1 Rev and cellular export receptor CRM1 (Lai et al., 2013); HCV by binding to the HCV core protein (Ariumi et al., 2007; Owsianka and Patel, 1999); and West Nile virus by binding to NS3 at viral replication sites (Chahar et al., 2013).

The New World alphavirus, Venezuelan equine encephalitis virus (VEEV) harbors a single stranded, positive sense RNA ranging ~11 kb in length that codes for 4 non-structural proteins (nsP1-4) from the genomic RNA and 5 structural proteins (capsid, envelope 3 (E3), E2, 6K and E1) from the subgenomic RNA (Foy et al., 2013a; Go et al., 2014). The structural proteins ultimately interact to form viral particles and the functions of the individual proteins are well understood (Atasheva et al., 2010a, 2010b; Foy et al., 2013a; Garmashova et al., 2007; Leung et al., 2011; Malygin et al., 2009; Parker et al., 2010; Snyder et al., 2013). The non-structural proteins (nsPs) are primarily responsible for viral replication (Foy et al., 2013a; Jose et al., 2009; Shin et al., 2012; Weaver and Barrett, 2004). We previously identified that VEEV-nsP3 interacts with the host kinase IKKβ in infected cells and that this interaction was important for efficient viral multiplication (Amaya et al., 2014). We

\* Corresponding author.

E-mail address: [anaraya1@gmu.edu](mailto:anaraya1@gmu.edu) (A. Narayanan).

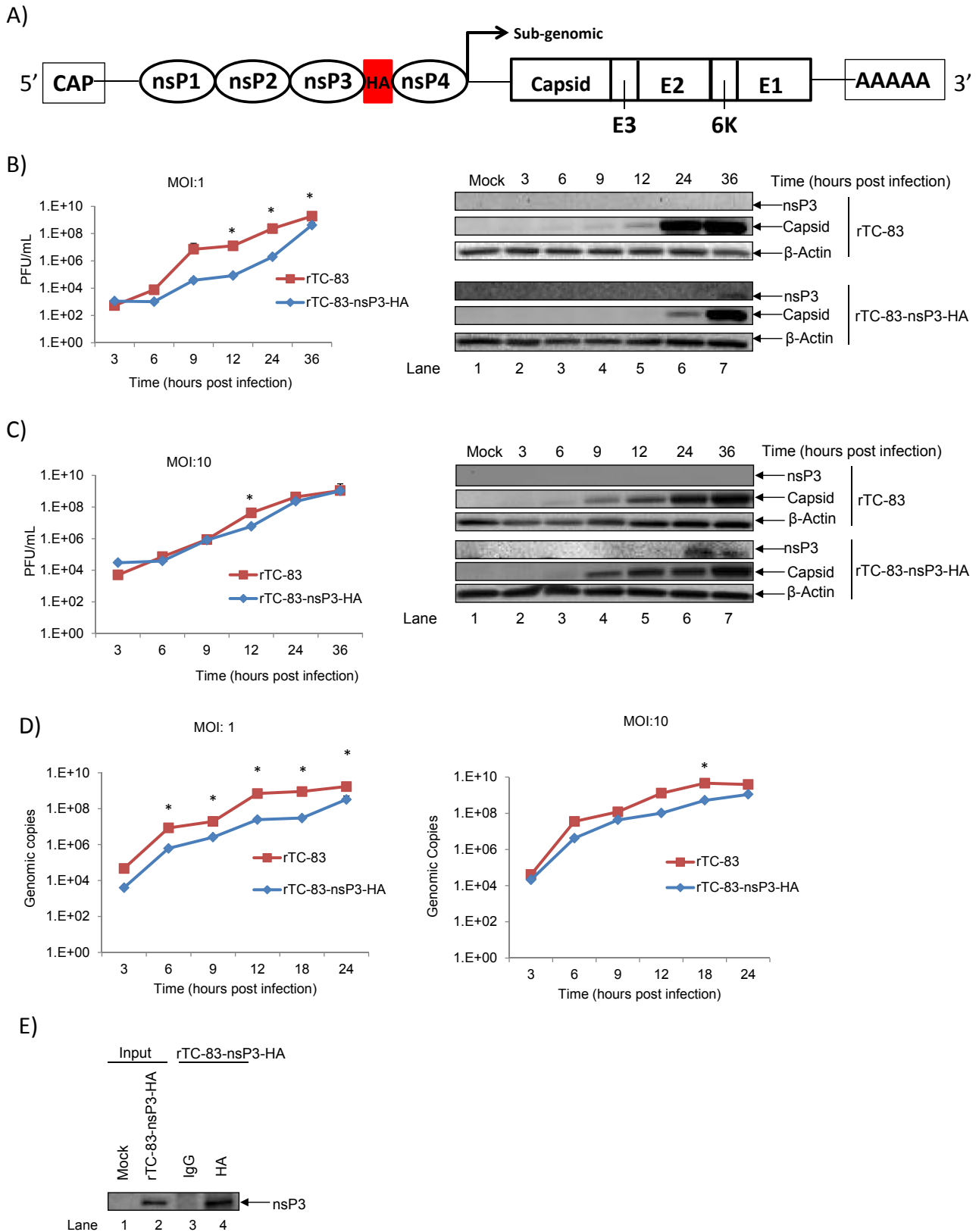


**Fig. 1. Replication kinetics of rTC-83-nsP3-HA is not altered with introduction of a HA tag.** A) Schematic representation of HA tag insertion in the rTC-83 background. Using the rTC-83 clone as a backbone and standard PCR recombination techniques, an HA tag was inserted at the C-terminus of nsP3 to allow for detection and isolation of nsP3-containing complexes. Briefly, the nsP3 region of rTC-83 was sub-cloned with primers containing a linker region (Ser-Ala-Ser-Ala) and an HA-tag was inserted at the C-terminal end of nsP3. The last residue of nsP3 was mutated from an alanine to a valine to prevent nsP2 cleavage of the tag. An initial stock of virus was prepared by electroporation of BHK-21 cells with rTC-83-nsP3-HA. U87MG cells seeded at a density of 10,000 cells per well in a 96 well plate were infected with rTC-83 or rTC-83-nsP3-HA at MOI:1 (B) and 10 (C) for 1 h. Fresh media were added to the cells and at 3, 6, 9, 12, 24 and 36 hpi supernatants were collected and analyzed by plaque assay for infectious viral particles. U87MG cells seeded at

hypothesized that VEEV-nsP3 interacts with a subset of host proteins in infected cells to form a VEEV-nsP3 interactome (molecular interactions of host proteins with VEEV-nsP3); such that knock-down of the identified host proteins will influence VEEV multiplication. We employed a mass spectrometry (MS) based approach from which RNA helicases, DDX1 and DDX3 were identified to interact with VEEV-nsP3 in infected cells. To assess the requirement for these interactions in the viral lifecycle, siRNA mediated depletion of DDX1 and DDX3 indicated a decrease in infectious viral titers. Therefore, our studies demonstrate a potential role for DDX1 and DDX3 in the VEEV life cycle. Collectively, these results will aid future studies of the role of VEEV-nsP3 in context of the viral life cycle.

## 2. Materials and methods

### 2.1. Viruses and cell lines

The live-attenuated virus TC-83 used in this study was obtained from BEI resources and virulent TrD was kindly provided by Dr. K. Kehn-Hall (George Mason University). Using the rTC-83 clone as a backbone and standard PCR recombination techniques, the nsP3 region of rTC-83 was sub-cloned with primers containing a linker region (Ser-Ala-Ser-Ala) and an HA-tag was inserted at the C-terminal end of nsP3. The last residue of nsP3 was mutated from an alanine to a valine to prevent nsP2 cleavage of the tag. The viral clone was confirmed with enzymatic digestion and sequencing. Primer sequences are available upon request. Human astrocytoma cells (U87MG cells), African green monkey kidney epithelial cells (VERO cells) and Baby Hamster Kidney-21 (BHK-21) cells were maintained in DMEM supplemented with 10% fetal bovine serum, 1% Penicillin/Streptomycin and 1% L-Glutamine at 37 °C, 5% CO<sub>2</sub>.

### 2.2. Immunoprecipitation and western blot

U87MG cells were infected with rTC-83-nsP3-HA at a multiplicity of infection (MOI) of 20. At 6 hours post infection (hpi) cells were collected and lysed in a buffer as previously described (Amaya et al., 2014, 2015). Two milligrams of total protein was utilized for immunoprecipitation using Dynabeads<sup>®</sup> protein G beads with antibodies to HA (Abcam, ab18181) or an isotype IgG control. The immunoprecipitates were washed 4× with TNE50 + 0.1% NP-40.

Preparation of whole cell lysates and western blot have been previously described (Amaya et al., 2014). Primary antibodies to HA, DDX1 (Abcam, ab31963), DDX3 (Cell Signaling, 2635), VEEV-capsid (BEI Resources, NR-9403), HRP conjugated actin, PABP (Santa Cruz Biotechnology, sc-28834), TIA-1 (Santa Cruz Biotechnology, sc-1751), eIF4G (Cell Signaling, C45A4) and eIF4A (Cell Signaling, C32B4) were used according to the manufacturer's instructions. The densitometric counts of the protein bands of interest were normalized to those of the actin bands and are illustrated graphically.

### 2.3. Liquid chromatography tandem mass spectrometry (LC-MS/MS)

U87MG cells were uninfected (Mock) or infected with rTC-83-

nsP3-HA (MOI:10). At 6 hpi cells were collected, lysed and processed as described for immunoprecipitation. Two milligrams of total protein was incubated overnight with rotation, at 4 °C with an isotype IgG control or HA antibodies. A 30% slurry of Protein A+G beads was added to the immunoprecipitates and incubated for 2 h with rotation at 4 °C. The immunoprecipitates were centrifuged briefly at 4 °C for 2 min at 2000 rpm and beads were washed 3× with TNE50 + 0.1% NP-40. LC-MS/MS analysis was carried out as previously described (Amaya et al., 2014; Narayanan et al., 2012).

### 2.4. Quantitative RT-PCR (q-RT-PCR)

At varying time points post infection U87MG cells were lysed using the MagMAX<sup>™</sup>-96 Total RNA Isolation Kit or MagMAX<sup>™</sup>-96 Viral RNA isolation kit as per the manufacturer's instructions. Viral RNA was quantitated using q-RT-PCR with primers and probe for nucleotides 7931–8005 of VEEV TC-83 (Kehn-Hall et al., 2012). Primer and probe pairs, q-RT-PCR assay and cycling conditions were previously described (Amaya et al., 2015). The absolute quantification was calculated based on the threshold cycle (Ct) relative to the standard curve.

### 2.5. siRNA knockdown experiments

U87MG cells were transfected with 10 nM of SMARTpool siRNAs against DDX1 (Dharmacon, M-011993-00-0005) and DDX3 (Dharmacon, M-006874-01-0005) using DharmaFECT 1 Transfection Reagent. As a negative control, a scrambled siRNA was included, siRNA-A (Santa Cruz Biotechnology, sc-37007). Transfected cells were infected with rTC-83 (MOI:0.1) at 48 h post transfection. At 6, 12 and 24 hpi, cells and supernatants were collected and analyzed by western blots, plaque assay or q-RT-PCR.

### 2.6. Inhibitor studies

The small molecule inhibitor was a kind gift from Dr. V. Raman (John Hopkins University). U87MG cells were pre-treated with RK-33 for 2 h and infected for 1 h. The viral inoculum was removed and replaced with media containing RK-33. At varying times post infection, supernatants were collected and analyzed by plaque assay.

### 2.7. Cell viability assay, plaque assay and immunofluorescence

Cell viability was measured using a Cell-Titer-Glo Luminescent Cell Viability kit as per the manufacturer's instructions and previously described in (Amaya et al., 2014, 2015). Cells were transfected with the control, DDX1 or DDX3 siRNAs or treated with varying concentrations of RK-33. Cell viability was determined at varying time points post transfection or treatment. Plaque assays were performed as previously described in (Amaya et al., 2015). Immunofluorescence assays were performed as previously described (Amaya et al., 2015).

### 2.8. Statistical analysis

Unless otherwise stated, graphs and images are the average of 2

30,000 cells per well in a 12 well plate were infected with rTC-83 or rTC-83-nsP3-HA at MOI:1 (B right), 10 (C right) for 1 h. Fresh media were added to the cells and at 3, 6, 9, 12, 24 and 36 hpi cell lysates were collected and analyzed by western blot for expression of nsP3, capsid and β-Actin. U87MG cells seeded at 10,000 cells per well in a 96 well plate were infected with rTC-83 or rTC-83-nsP3-HA at MOI:1 (D right) and 10 (D left) for 1 h. Fresh media were added to the cells and at 3, 6, 9, 12, 18 and 24 hpi cells were lysed with MagMAX<sup>™</sup>-96 Total RNA Isolation Kit. Levels of viral RNA were quantified by q-RT-PCR using VEEV specific primers. E) U87MG cells were uninfected (Mock) or infected with rTC-83-nsP3-HA at MOI:20 for 1 h. Fresh media were added to the cells and at 6 hpi cell lysates were collected and quantified by Bradford assay. Dynabeads protein G beads was used for immunoprecipitation of 2 mg total protein with a HA antibody or an IgG isotype control antibody. The immunoprecipitates were resolved by SDS-PAGE and the subsequent western blot was probed with an HA antibody. The graphs represent an average of 2 independent experiments where each experiment was performed in triplicate. Western blots were performed as 3 independent experiments. Standard deviations were calculated accordingly. \* =  $p \leq 0.05$ .

A)

|    | Reference   | Score    | MW       | Accession |
|----|---|----------|----------|-----------|
|    | Scan(s)   | XC       | Sp       | RSp       |
| 1  | DEAD/H (Asp-Glu-Ala-Asp/His) box polypeptide 3 [Homo sapiens]           | 20.2     | 73198.13 | 87196351  |
| 2  | DEAD (Asp-Glu-Ala-Asp) box polypeptide 1 [Homo sapiens]                 | 10.30474 | 82379.86 | 4826686   |
| 3  | microtubule-associated protein 1B [Homo sapiens]                        | 280.3051 | 270465.9 | 153945728 |
| 4  | plectin 1 isoform 1 [Homo sapiens]                                      | 10.19741 | 518156.3 | 47607492  |
| 5  | fragile X mental retardation-related protein 1 isoform a [Homo sapiens] | 40.24046 | 69677.98 | 61835148  |
| 6  | heterogeneous nuclear ribonucleoprotein A1-like [Homo sapiens]          | 20.27079 | 34204.26 | 58761496  |
| 7  | ribosomal protein S8 [Homo sapiens]                                     | 30.29645 | 24190.17 | 4506743   |
| 8  | ribosomal protein P0 [Homo sapiens]                                     | 50.21938 | 34251.79 | 16933546  |
| 9  | ribosomal protein L10a [Homo sapiens]                                   | 20.22554 | 24815.54 | 15431288  |
| 10 | ribosomal protein L6 [Homo sapiens]                                     | 10.17011 | 32707.63 | 16753227  |

B)

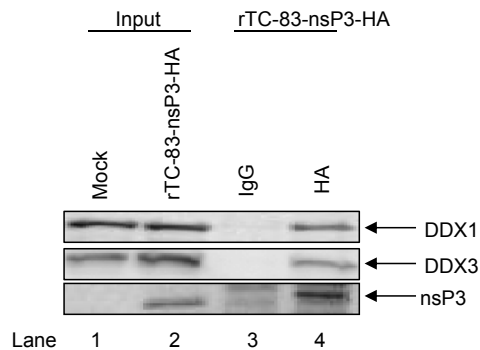


**Fig. 2. VEEV-nsP3 associates with DDX1 and DDX3.** A) U87MG cells were uninfected (Mock) or infected with rTC-83-nsP3-HA (MOI:10) for 1 h. Fresh media were added to the cells and at 6 hpi cell lysates were collected and quantified. Two milligrams of total protein from each sample was immunoprecipitated with an HA antibody or an isotype IgG control antibody. The immunoprecipitates were processed for LC/MS-MS. A total of 3 independent experiments were performed and each MS run was performed in duplicate to generate a data set that was compared and contrasted for unique proteins identified only in the rTC-83-nsP3-HA infected samples immunoprecipitated with HA. The identified proteins were tiered based on at least 50% reproducibility and additionally tiered according to peptide hits. B) U87MG cells were infected with rTC-83-nsP3-HA (MOI:20) for 1 h. Fresh media were added to the cells and at 6 hpi cell lysates were collected and quantified. Two milligrams of total protein was immunoprecipitated with an isotype IgG control or an HA antibody. The immunoprecipitates were resolved by SDS-PAGE and the subsequent immunoblot probed with antibodies to DDX1, DDX3 or HA. The western blot is a representative image of 2 independent experiments.

independent experiments. Independent experiments were performed in triplicate. All experimental results were expressed as the arithmetic mean. Standard deviations were calculated and represented thusly. All statistical analyses were performed with the unpaired, two-tailed Student T-test using GraphPad's - QuickCalcs software (GraphPad).

### 3. Results

#### 3.1. Characterization of rTC-83-nsP3-HA

Using rTC-83 as a backbone, an HA tag was inserted at the C-terminus of nsP3 (Fig. 1A), rTC-83-nsP3-HA, to allow for detection and isolation of nsP3-containing complexes. The replication kinetics of rTC-83 and rTC-83-nsP3-HA in U87MG cells at a low (MOI:1) and high (MOI:10) MOI were compared to determine if insertion of the tag significantly impaired viral replication. Relative titers of infectious virus analyzed by plaque assay indicated that at the low MOI a minor lag in the replication kinetics was observed

(Fig. 1B left) but at the higher MOI the replication kinetics of the tagged virus was comparable to that of the wild type rTC-83 (Fig. 1C left). Expression levels of the structural protein capsid (representative for viral protein expression) of rTC-83-nsP3-HA were comparable to that of rTC-83 (Fig. 1B and C, right). We determined nsP3 protein expression by virtue of the HA tag in whole cell extracts at later time points at the higher MOI (Fig. 1C, right, lanes 6 and 7). We next determined if insertion of the HA tag impacted intracellular viral RNA kinetics by q-RT-PCR using VEEV specific primers. Fig. 1D indicated that rTC-83-nsP3-HA replicated to high titers over the time course investigated in an MOI dependent manner when compared to rTC-83. Western blot analysis demonstrated that nsP3 could be immunoprecipitated by using the tag from infected cells at 6 hpi (Fig. 1E, lane 4). We also validated the IKK $\beta$ :nsP3 interaction that we had reported in our previous publication using a plasmid construct that expressed nsP3 (Amaya et al., 2014) (Fig. S1A). Additionally, our confocal microscopy studies illustrated VEEV-nsP3 localizing as distinct cytoplasmic structures (as reported by others (Foy et al., 2013a, 2013b)). Within these structures, we were

also able to observe localization of IKK $\beta$  at 12 hpi (Fig. S1B). Overall, rTC-83-nsP3-HA could replicate to high titers and appropriately express viral proteins. Taken together these results indicate that rTC-83-nsP3-HA can be utilized as a tool to yield biologically relevant data.

### 3.2. VEEV-nsP3 interacts with DDX1 and DDX3

A mass spectrometry (MS) based approach was taken to identify host proteins that interact with VEEV-nsP3. U87MG cells were uninfected (Mock) or infected with rTC-83-nsP3-HA (MOI: 10) and at 6 hpi cells were collected, lysed and quantified. Total protein was immunoprecipitated with an HA antibody or an isotype IgG control antibody and processed for LC-MS/MS. MS spectra and identified peptides were searched against the NCBI human protein database. Identified host proteins from rTC-83-nsP3-HA samples were cross referenced with the Mock (IgG and HA) samples and the rTC-83-nsP3-HA (IgG) samples to identify unique candidates in the infected group. Proteins that reproduced in at least 3 out of the 6 individual sample sets that were independently subjected to MS analyses were tabulated (Fig. 2A). Among the proteins identified, we focused our attention on the helicases DDX1 and DDX3 based on the rationale that nsP3 functionality is likely to be important to assist in viral RNA replication and protein expression (Galbraith et al., 2006; Lastarza et al., 1994; Wang et al., 1994). Therefore, RNA helicases DDX1 and DDX3 (Table 1, red box (in the web version)) were considered for further validation.

Co-immunoprecipitation was performed to validate the interactions between VEEV-nsP3 and DDX1 and DDX3. Western blot analysis indicated an interaction of DDX1 and DDX3 with VEEV-nsP3 (Fig. 2B, lane 4) in infected cells. As an additional level of validation, confocal microscopy was performed using DDX1 and DDX3 antibodies. These two proteins had a very broad cytoplasmic localization in the cells as revealed by confocal imaging with observable co-localization of DDX1:nsP3 and DDX3:nsP3 (Fig. S2). These data indicate that VEEV-nsP3 interacts with DDX1 and DDX3 in infected cells.

### 3.3. DDX1 and DDX3 facilitate rTC-83 replication

To determine the influence of the DDX1:nsP3 and DDX3:nsP3 interactions on viral multiplication, depletion analyses were performed. Initially, U87MG cells were transfected with a smartpool of siRNAs against DDX1 and DDX3 to determine the optimum time point for efficient knockdown of the target proteins. As a negative control a scrambled siRNA (control siRNA) was included. Transfected cells were collected at 24, 48 and 72 h post transfection and lysed. Western blot analysis indicated that silencing of DDX1 and DDX3 was efficient as early as 48 h post transfection (Fig. 3A left and right respectively), with ~90% and ~95% loss, respectively, when compared to the control. Depletion of either protein did not indicate a significant decrease in cell viability (Fig. 3B). As such downstream assays were conducted at 48 h post transfection.

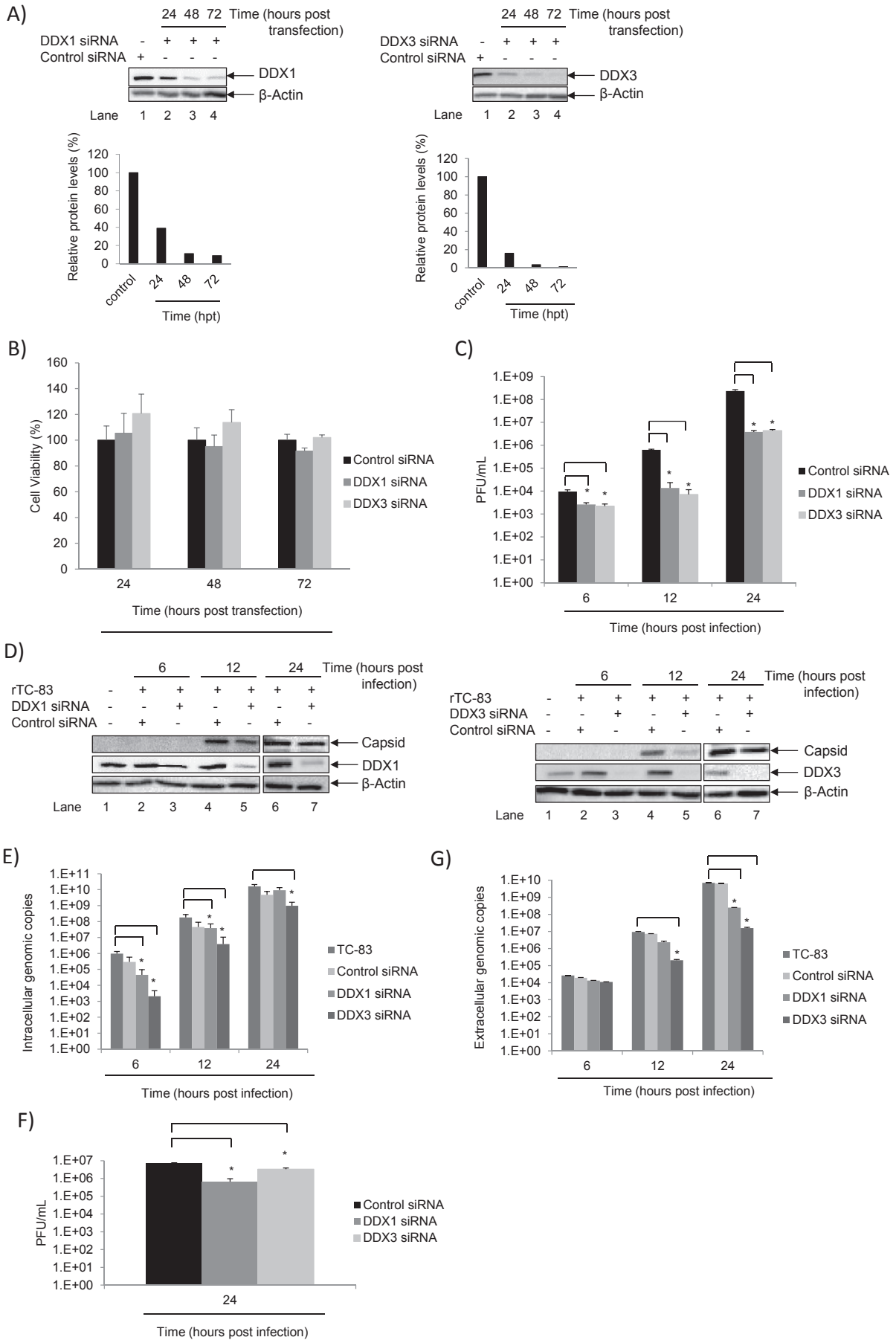
To determine the impact of depleting either DDX1 or DDX3 on viral multiplication, U87MG cells transfected with control, DDX1 or DDX3 siRNA were infected with rTC-83. Supernatants were collected at 6, 12 and 24 hpi and analyzed by plaque assay for infectious virions. In the DDX1 and DDX3 depleted infected cells, a ~70% decrease in infectious viral titers was observed at 6 hpi, whereas at 12 hpi and 24 hpi, a ~1log and 2log decrease in infectious viral titers was observed, respectively (Fig. 3C), suggesting a

time dependent decrease in infectious viral titers in DDX1 and DDX3 depleted cells. Cell lysates from the experiment performed in Fig. 3C were collected and resolved by SDS-PAGE. The subsequent blot was probed for VEEV capsid, DDX1, DDX3 and  $\beta$ -actin (Fig. 3D). Western blot analysis indicated that VEEV capsid levels were modestly reduced in DDX1 (Fig. 3D left) and DDX3 (Fig. 3D right) depleted cells when compared to the control. Capsid protein expression could not be detected as early as 6 hpi by western blot. In addition, intracellular and extracellular viral RNA was quantified by q-RT-PCR using VEEV specific primers. DDX1 or DDX3 depleted U87MG cells infected with rTC-83 were processed for q-RT-PCR at 6, 12 and 24 hpi. In DDX1 depleted cells a 1log decrease was observed at 6 and 12 hpi was observed whereas at 24 hpi a 50% decrease was observed in intracellular viral RNA replication when compared to the controls (Fig. 3E). A 2log decrease in intracellular viral RNA replication was observed at 6 and 12 hpi, and a 1log decrease was observed at 24 hpi in the DDX3 depleted cells when compared to the controls. It was observed in DDX1 depleted cells at 6, 12 and 24 hpi a 50%, 70% and a 1log decrease in extracellular viral RNA replication, respectively (Fig. 3F). In DDX3 depleted cells a ~1log decrease in extracellular viral RNA was observed at 6 and 12 hpi, whereas at 24 hpi a 2log decrease was observed when compared to the rTC-83 controls. Taken together, depletion of endogenous DDX1 and DDX3 at non-toxic concentrations resulted in a significant decrease in rTC-83 replication. This suggests that these RNA helicases positively regulate VEEV replication potential, with potentially, DDX3 having a comparatively greater impact on VEEV life cycle in the context of TC-83.

We next determined if DDX1 and DDX3 contribution extended to the multiplication potential of virulent VEEV, TrD. Here supernatants were collected at 24 hpi from infected U87MG cells transfected with control, DDX1 or DDX3 siRNAs to be analyzed by plaque assay. Fig. 3G demonstrated a ~1log decrease with DDX1 siRNA, whereas ~55% decrease in viral titers was observed with DDX3 siRNA when compared to the control. From Fig. 3G it appears that although TrD multiplication was inhibited similar to that seen with rTC-83 at 24 hpi, the extent of inhibition differed by 1log, which may speak to the difference in viral virulence between the two strains. This data suggests that the virulent TrD strain utilizes DDX1 and DDX3 for viral multiplication although, the reliance on DDX3 may be lesser for the virulent strain. Collectively, the data indicates that VEEV utilizes DDX1 and DDX3 to facilitate viral replication.

### 3.4. DDX1/DDX3 double knockdown down regulates rTC-83 replication

Viruses such as HIV-1 (Edgcomb et al., 2012; Lai et al., 2013; Yasuda-Inoue et al., 2013) and HCV (Ariumi et al., 2007; Owsianka and Patel, 1999; Tingting et al., 2006) utilize both DDX1 and DDX3 to facilitate viral replication; likewise, in our studies, VEEV-nsP3 interacted with both DDX1 and DDX3. This opens the possibility that RNA helicases may serve compensatory roles in the viral life cycle. To address this we hypothesized that depletion of both DDX1 and DDX3 would result in a greater decrease in infectious viral titers than that observed in the individual depletion studies. Western blot analysis indicated that silencing of DDX1 and DDX3 was highly efficient as early as 48 h post transfection (Fig. 4A) at non-toxic concentrations (Fig. 4B). To determine the impact of depleting both DDX1 and DDX3 on viral multiplication, U87MG cells transfected with control or DDX1 and



DDX3 siRNA were infected with rTC-83 and supernatants were collected at 6, 12 and 24 hpi. Plaque assay analysis indicated that in the DDX1/3 depletion scenario a 1log decrease in viral titers was observed at 6 hpi and 24 hpi, whereas at 12 hpi a 2log decrease in infectious viral titers was observed when compared to the respective controls (Fig. 4C). The decrease observed in infectious viral titers using the combinatorial knockdown was modestly greater than with the individual knockdowns at 6 and 12 hpi, suggesting that DDX1 and DDX3 are more likely to serve compensatory functions in VEEV multiplication. Although the decrease in infectious viral titers observed at 24 hpi was with the double knockdown was statistically significant, it was not greater than the individual knockdowns. In addition, intracellular capsid protein expression in the siRNA studies was assessed under the same experimental conditions as Fig. 4C. Western blot analysis indicated that in comparison to the respective controls, at 12 hpi and 24 hpi capsid protein expression was reduced with DDX1/3 siRNA (Fig. 4D). In addition, intracellular and extracellular viral RNA was quantified by q-RT-PCR. DDX1 or DDX3 depleted U87MG cells infected with rTC-83 were processed for q-RT-PCR at 6, 12 and 24 hpi. Fig. 4E indicated that at 6 and 24 hpi a 1log decrease in intracellular viral RNA replication was observed when compared to the rTC-83 controls, whereas at 12 hpi a 2log decrease was observed. Fig. 4F indicated that extracellular viral RNA was decreased by 2logs at 12 and 24 hpi, however, no significant decrease (30%) was observed at 6 hpi when compared to the rTC-83 controls. This observation leads us to speculate that the dependence on host RNA helicases may be more prominent in the context of these infected cells, at the later time points during infection when iterative rounds of viral multiplication have occurred in the infected cells. This may also be related to the relative abundance of viral multiplication in the cells that may impose additive demands on the host machinery to support a productive viral infection. To determine if DDX1 and DDX3 double knockdown extended to TrD, supernatants collected at 24 hpi from infected U87MG cells transfected with control or DDX1/3 siRNAs were analyzed by plaque assay for infectious virions. Fig. 4G demonstrated a ~1log decrease with DDX1/3 siRNA when compared to the control. Taken together this data reiterates that TC-83 is likely to utilize DDX1 and DDX3 for viral multiplication.

### 3.5. VEEV-nsP3 associates with eukaryotic translation initiation machinery in infected cells

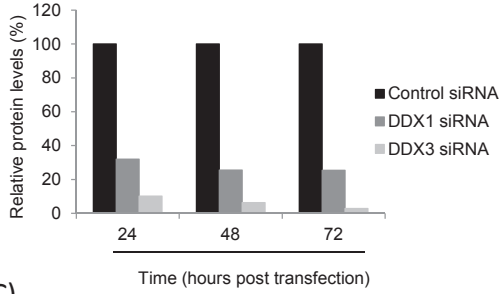
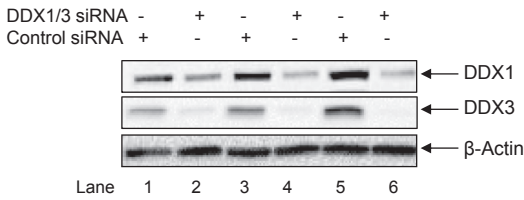
Upon conditions of a cellular stress response, the cell organizes assembled preinitiation complexes into stress granules (SGs) (Lloyd, 2012; Scholte et al., 2015), which comprise numerous components such as: eukaryotic initiation factor (eIF)3, eIF4F

(comprising eIF4E, eIF4A and eIF4G), eIF4B, small ribosomal subunits and poly A binding protein-1 (PABP-1) (Anderson and Kedersha, 2008; Buchan and Parker, 2009; Scholte et al., 2015), T cell internal antigen-1 (TIA-1) and TIA-1-related (TIAR), and fragile X mental retardation protein (Anderson and Kedersha, 2008; Buchan and Parker, 2009; Scholte et al., 2015), G3BP1 and G3BP2 (Anderson and Kedersha, 2008; Buchan and Parker, 2009). These components are universal markers for SGs. Multiple viruses and viral proteins such as, Junin virus (Linerio et al., 2013), Rotavirus NSP3A (Piron et al., 1998), Herpes simplex virus immediate early ICP27 protein (Fontaine-Rodriguez et al., 2004) and Influenza virus NS1 and PABP (Burgui et al., 2003) have been shown to interact with host eIFs to aid in viral multiplication. Old world alphaviruses SFV (Panat et al., 2012), SINV and CHIKV (Fros et al., 2012) have been shown to induce SG formation in G3BP1 foci early in infected cells and interact with G3BPs (Fros et al., 2012; Panat et al., 2012; Scholte et al., 2015). In particular SFV-nsP3 recruits G3BP and disassembles SGs (Scholte et al., 2015). Although studies involving new world alphavirus association with SGs are limited; what is known is that VEEV-nsP3 does not associate with G3BPs (Foy et al., 2013a).

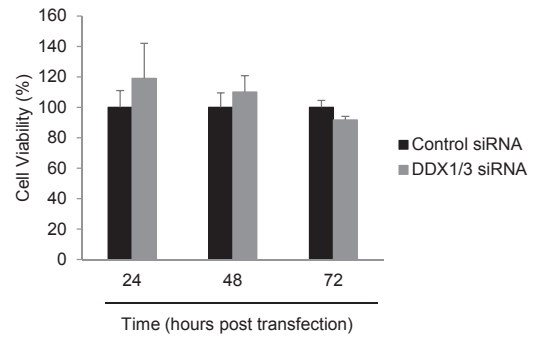
DDX3 was observed to localize in SGs (Ariumi, 2014; Lai et al., 2013), where it associates with eIF4A, eIF4G, eIF2a, eIF3 and PABP to facilitate translation of mRNA containing structured 5' UTR (Ariumi, 2014; Lai et al., 2013; Shih et al., 2012). Of note, in our MS analysis, we also identified PABP as interacting with nsP3; however PABP fell below our condition of 50% reproducibility and therefore excluded from Fig. 2A. We hypothesized that the interaction of DDX3 with nsP3 may play a role in facilitating the recruitment of the eIF machinery to potentially aid in translation of viral proteins. Therefore, we asked, does VEEV-nsP3 associate with any of the eIFs that are known to interact with DDX3? To address this we proposed the following working model (Fig. 5A). During VEEV infection, a global inhibition of cellular transcription and translation occurs (Akhrymuk et al., 2012), resulting in accumulation of pre-existing DDX3-eIF4A-eIF4G-PABP complexes. We propose that VEEV-nsP3 interacts with DDX3 along with its pre-existing partners to initiate translation of viral mRNA. To address the validity of this model, U87MG cells infected with rTC-83-nsP3-HA (MOI:20) were collected at 6 hpi, lysed and processed for immunoprecipitation. The subsequent western blot was probed with antibodies to HA, eIF4A, eIF4G, PABP and DDX3. Fig. 5B illustrates that VEEV-nsP3 interacts with the host translational factors; eIF4A, eIF4G and PABP; together with DDX3 thus supporting our proposed working model. Taken together, this data puts forth the suggestion that VEEV-nsP3 may co-opt the host translational machinery from SGs to initiate translation of viral proteins in infected cells.

**Fig. 3. Depletion of DDX1 and DDX3 decreases rTC-83 multiplication.** U87MG cells were transfected with 10 nM of control siRNA, DDX1 siRNA or DDX3 siRNA. A) At 24, 48 and 72 h post transfection cell lysates were collected and resolved by SDS-PAGE. The subsequent blot was probed for DDX1 in the case of DDX1 siRNA transfectants (left panel) or DDX3 with the DDX3 siRNA transfectants (right panel). As a loading control the blots were probed with  $\beta$ -actin. Densitometric counts for DDX1, DDX3 and  $\beta$ -actin were obtained using the Quantity One Analysis Software. The normalized data are represented graphically below the respective western blot images. The western blot images are representative of 2 independent experiments. B) Cell viability assay was performed at 24, 48 and 72 h post transfection using the Cell Titer Glo Luminescent Cell Viability Assay according to the manufacturer's instructions. The graph is representative of 3 independent experiments performed in triplicate and is depicted as a percentage of cell viability. C) At 48 h post transfection, U87MG cells were infected with rTC-83 (MOI:0.1) for 1 h. Fresh media were added to the cells and at 6, 12 and 24 hpi supernatants were collected and analyzed by plaque assay. The graph is representative of 2 independent experiments performed in triplicate. D) At 48 h post transfection, U87MG cells were infected with rTC-83 (MOI:0.1) for 1 h. Fresh media were added to the cells and at 6, 12 and 24 hpi cell lysates were collected and resolved by SDS-PAGE. The subsequent blot was probed for capsid and DDX1 in the case of DDX1 siRNA transfectants (left panel) or capsid and DDX3 with the DDX3 siRNA transfectants (right panel). As a loading control the blots were probed for  $\beta$ -actin. The 24 hpi blots are depicted separately as these were imaged at a shorter exposure. The images are representative of 2 independent experiments. DDX1, DDX3 or control siRNA were used to transfect U87MG cells seeded at 10,000 cells per well in a 96 well plate. Transfected cells were infected with rTC-83 (MOI:0.1) for 1 h. Fresh media were added to the cells and at 6, 12 and 24 hpi cells were lysed with MagMAX™-96 Total RNA Isolation Kit (E) or MagMAX™-96 Viral RNA isolation kit (F). Levels of viral RNA were quantified by q-RT-PCR using VEEV specific primers. The graphs are representative of 2 independent experiments, each performed in triplicate. G) U87MG cells were transfected with 10 nM of control siRNA, DDX1 or DDX3 siRNA. At 48 h post transfection, U87MG cells were infected with VEEV TrD (MOI:0.1) for 1 h. Fresh media were replaced after the infection and at 24 hpi supernatants were collected and analyzed by plaque assay. The graph is representative of a biological duplicate experiment each as technical triplicates and is depicted as percent infectious viral titers. \* =  $p \leq 0.05$ . ND = not detectable.

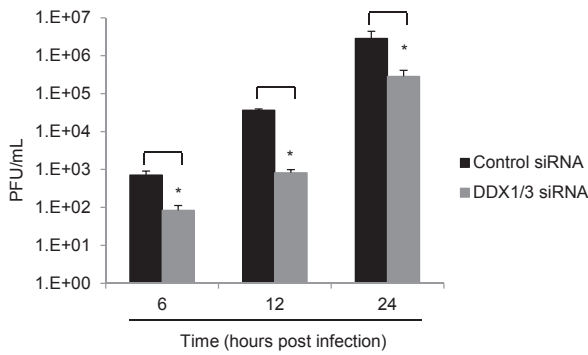
**A)** 24 48 72 Time (hours post transfection)



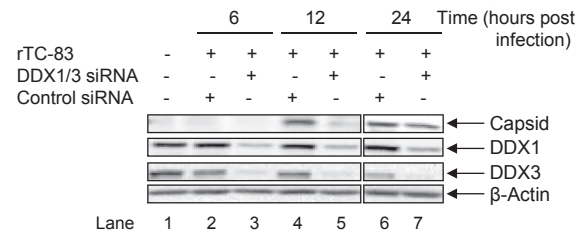
**B)**



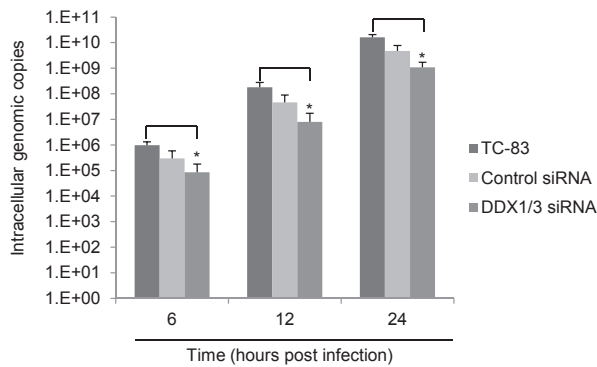
**C)**



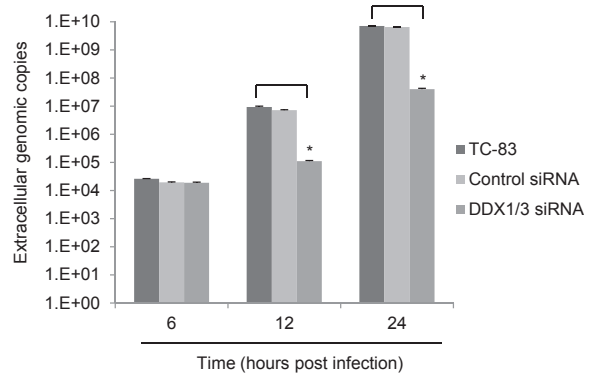
**D)**



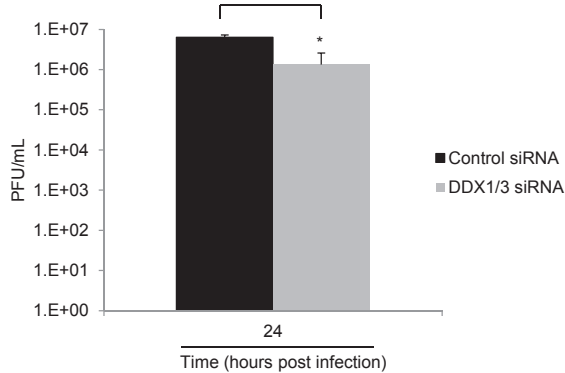
**E)**



**F)**



**G)**



### 3.6. RK-33 disrupts VEEV-nsP3 interactions with eukaryotic translation initiation machinery

The small molecule, RK-33 was designed to specifically bind to the ATP-binding cleft of DDX3 to inhibit the helicase unwinding activity (Bol et al., 2015). We asked if inhibiting DDX3 helicase activity would have an effect on the interactions between VEEV-nsP3 and the identified host translational components. We initially determined by cell viability assays the highest non-toxic concentration of RK-33 (1  $\mu$ M) (Fig. 6A). Next we determined if RK-33 interfered with viral RNA replication kinetics over a time course. Plaque assay analyses indicated that at 8 and 16 hpi a 1log decrease in infectious viral titers was observed when compared to the DMSO controls (Fig. 6B). However, at 4 hpi no observable difference occurred in the RK-33 treated cells whereas at 24 hpi a 50% reduction in infectious viral titers was observed when compared to the DMSO control. Hence, we opted for a 6 hpi time point to determine if inhibition of DDX3 helicase activity interfered with the interactions between VEEV-nsP3 and the host translational components, as the inhibitor treatment at this time point would not interfere with viral replication kinetics. Western blot analysis indicated a decrease in interactions between VEEV-nsP3 and eIF4G, eIF4A and PABP (Fig. 6C, compare lanes 5 and 7). This decrease was not due to reduced levels of VEEV-nsP3. Densitometric counts indicated that VEEV-nsP3 interactions with eIF4G, eIF4A and PABP were reduced by 54%, 86% and 44% respectively. This data indicates that DDX3 helicase activity may be necessary for VEEV-nsP3 interactions with host translational machinery to potentially facilitate viral translation.

## 4. Discussion

This study aimed to use VEEV as a prototypical representative of new world alphaviruses to characterize the VEEV-nsP3 interactome and determine the consequence of the interactions on viral multiplication in the context of a model human glioblastoma cell line. The introduction of an HA tag at the C-terminal end of rTC-83 (rTC-83-nsP3-HA) did not significantly impede viral replication kinetics (Fig. 1) and could therefore be utilized as a tool to characterize the VEEV-nsP3 interactome. We identified and validated RNA helicases, DDX1 and DDX3 as interacting partners of VEEV-nsP3 (Fig. 2). DDX1 and DDX3 were found to have an effect on rTC-83 multiplication (Figs. 3 and 4). Although we observed a similar decrease in TrD multiplication when compared to rTC-83, the extent of inhibition differed by a log, which may speak to the difference in virulence between the two strains. The U87MG glioblastoma cell model is an attractive system to study host-based candidates for development of therapeutics against alphavirus infections. Additional studies with primary brain cells will enable us to further our understanding of the magnitude of relevance of

DDX1 and DDX3 to new world alphavirus infections.

The dependence of new world alphaviruses on host-derived helicases poses an interesting concept to the interactions of VEEV with the human host. While other viruses such as HIV and influenza have been demonstrated to utilize DDX3 as part of their infectious cycle, the fact that new world alphavirus nsP2 protein exhibits helicase activity on its own raises the question regarding the magnitude of dependence on host-based helicase activity. To that effect, we have observed that the dependence of the virulent TrD strain on DDX3 is lesser than that of TC-83 (Fig. 4), which may also attest to the dependence on host helicases as a reflection of viral virulence.

Based on DDX3 and DDX1 function in unwinding RNA secondary structures it is worth considering that VEEV-nsP3 co-opts DDX1 and DDX3 at early stages of infection to assist in unwinding of the viral RNA to initiate replication and/or translation. This suggests that RNA helicases may serve redundant roles in the viral life cycle or may be utilized at different time points in the viral life cycle to serve different roles. On that note, it is important to bear in mind that during the course of infection, different pools of VEEV-nsP3 may be present that interact with a selected subset of host proteins, which may speak to VEEV-nsP3 interacting with DDX1 and DDX3 at different times during infection to serve different roles in the viral life cycle. This may offer a plausible explanation to the additive effect of the double knockdown scenario where a decrease in infectious viral titers was greater than that observed with the individual knockdowns at the earlier time points of infection (Figs. 3C and 4C); however, at 24 hpi similar levels of infectious viral titers were detected between the individual and combinatorial knockdowns. Determining if DDX1 and/or DDX3 are required for synthesis of (+) RNA, (–) RNA or subgenomic viral RNAs or translation of viral RNA is a future avenue being explored in our laboratory.

We proposed a working model to provide a mechanistic explanation for VEEV-nsP3 interactions with DDX3 and the requirement of this interaction for viral multiplication (Fig. 5A). We demonstrated that VEEV-nsP3 interacts with translation initiation factors eIF4A, eIF4G and PABP (Fig. 5B), indicating that VEEV-nsP3 subverts the pre-formed eIF4F-DDX3 complex in infected cells to potentially initiate translation of viral proteins. Addition of the small molecule inhibitor, RK-33 demonstrated a significant reduction in VEEV-nsP3 interactions with the host translational machinery (Fig. 6C), suggesting that DDX3 helicase activity may be needed for these protein:protein interactions.

There appears to be differential requirements of DEAD box proteins DDX1 and DDX3 by different viruses as evidenced by the observations with HIV-1, influenza, and now VEEV. In the case of HIV-1, DDX1 and DDX3 are critical co-factors that interact with HIV-1 Tat and Rev to promote HIV-1 mRNA translation and transition to late-stage HIV-1 infection (Lai et al., 2013). A recent study

**Fig. 4. Double knockdown of DDX1 and DDX3 reduced rTC-83 multiplication.** U87MG cells were transfected with 10 nM of control siRNA or with a combination of 10 nM of DDX1 and DDX3 siRNA. A) At 24, 48 and 72 h post transfection cell lysates were collected and resolved by SDS-PAGE. The subsequent blot was probed for DDX1 and DDX3. As a loading control the blots were probed with  $\beta$ -actin. Densitometric counts for DDX1, DDX3 and  $\beta$ -actin were obtained using the Quantity One Analysis Software. The normalized data are represented graphically below the western blot image. B) Cell viability assay was performed at 24, 48 and 72 h post transfection using the Cell Titer Glo Luminescent Cell Viability Assay according to the manufacturer's instructions. The graph is representative of 3 independent experiments performed in triplicate and is depicted as a percentage of cell viability. C) At 48 h post transfection, U87MG cells were infected with rTC-83 (MOI:0.1) for 1 h. Fresh media were added to the cells and at 6, 12 and 24 hpi supernatants were collected and analyzed by plaque assay. The graph is representative of 2 independent experiments performed in triplicate. D) At 48 h post transfection, U87MG cells were infected with rTC-83 (MOI:0.1) for 1 h. Fresh media were added to the cells and at 6, 12 and 24 hpi cell lysates were collected and resolved by SDS-PAGE. The subsequent blot was probed for capsid, DDX1, or DDX3. As a loading control the blots were probed with  $\beta$ -actin. The 24 hpi blots are depicted separately as these were imaged at a shorter exposure. The images are representative of 2 independent experiments. DDX1, DDX3 or control siRNA were used to transfect U87MG cells seeded at 10,000 cells per well in a 96 well plate. Transfected cells were infected with rTC-83 (MOI:0.1) for 1 h. Fresh media were replaced after the infection and at 24 hpi supernatants were collected and analyzed by plaque assay. The graph is representative of a biological duplicate experiment each as technical triplicates and is depicted as percent infectious viral titers. \* =  $p \leq 0.05$ . ND = not detectable.

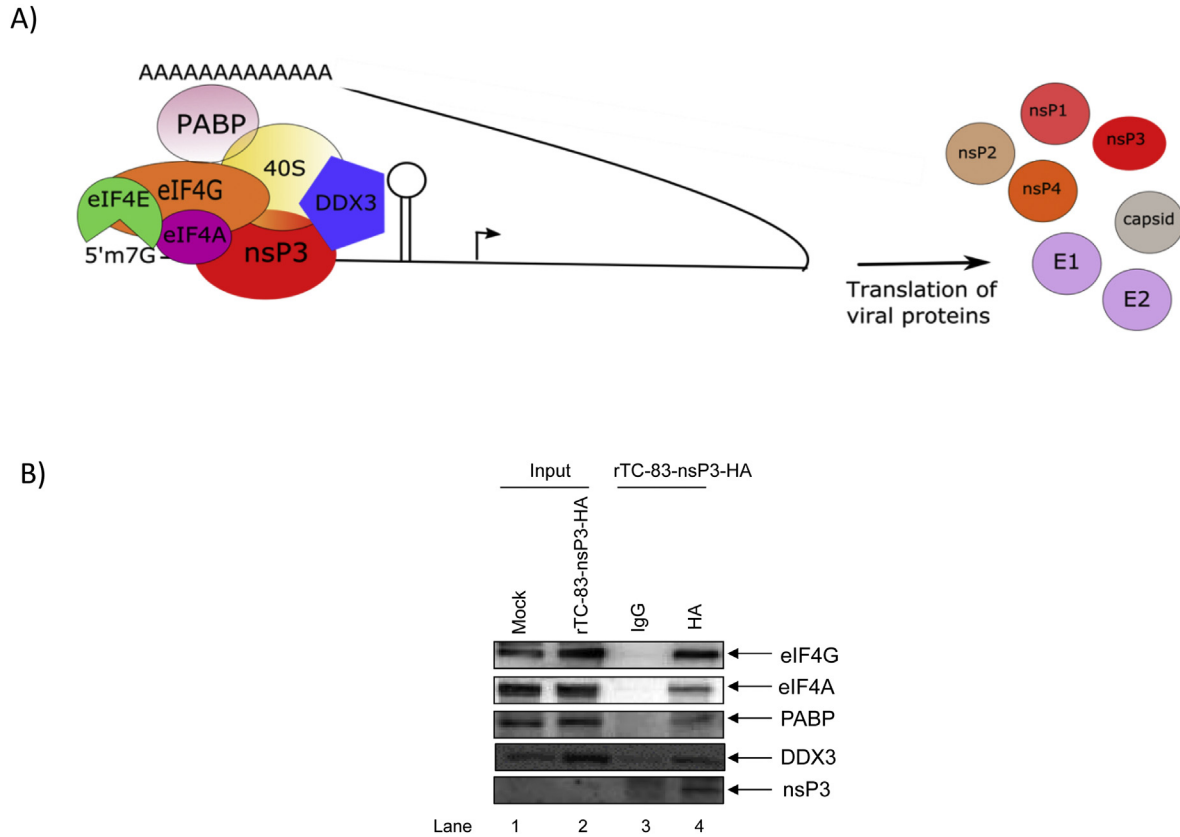


**Fig. 5. VEEV-nsP3 interacts with components of the host translational machinery.** A) Working model for VEEV-nsP3 interaction with eukaryotic initiation factors. During shut off of cellular transcription and translation pre-existing DDX3, eIF4A, eIF4G and PABP complexes are stalled in cytoplasmic SGs. During VEEV infection, VEEV-nsP3 interacts with these pre-existing complexes to initiate translation of viral mRNA. eIF4E initially recognizes 5' methylguanosine caps on VEEV RNA and then complexes with eIF4A (helicase) and eIF4G (scaffold protein) to form the eIF4F complex, which then recruits the 40S ribosome. PABP binds to the poly(A) tail present at the 3'-end of VEEV RNA circularizing VEEV RNA. B) U87MG cells were infected with rTC-83-nsP3-HA (MOI:20) for 1 h. At 6 hpi cell lysates were collected, quantified and 2 mg of total protein was immunoprecipitated with an isotype IgG control or an HA antibody. The immunoprecipitates were resolved by SDS-PAGE and the subsequent immunoblot probed with antibodies to eIF4A, eIF4G, PABP, DDX3 or HA. The western blot is a representative image from 2 independent experiments.

demonstrated that DDX3 interacted with influenza virus NS1 and NP proteins, and localized to virus induced SGs (Thulasi Raman et al., 2016). Furthermore, that study indicated that DDX3 is capable of nucleating stress granule formation, and that the core helicase domain of DDX3 was sufficient for its localization to SGs (Thulasi Raman et al., 2016). This offers further support to the loss of interactions we observed between VEEV-nsP3 and the host translational machinery with treatment of RK-33. Alternatively, VEEV-nsP3 could usurp these host factors to disassemble the SGs to create an environment suitable for efficient viral multiplication. A similar subversion of SGs is necessary for establishment of a successful influenza infection, as knockdown of DDX3 impaired stress granule formation and increased viral titers (Thulasi Raman et al., 2016). The effect of VEEV-nsP3 interactions with host translational machinery on viral translation are future avenues being explored by our laboratory.

The applicability of DEAD box proteins as candidates for therapeutic intervention has primarily been researched in the field of cancer biology. DDX3 levels have been observed to be significantly elevated in a number of human sarcoma subtypes (Wilky et al., 2015). Treatment with the small molecule inhibitor RK-33 was found to be preferentially cytotoxic to sarcoma cells, including chemotherapy resistant cells, but spared non-malignant cells (Wilky et al., 2015). It was also reported that 39% of all colorectal tumors overexpressed DDX3 (Heerma van Voss et al., 2015). Knockdown of DDX3 function in colorectal tumors with RK-33 was

reported to cause G1 cell cycle arrest, reduced tumor proliferation, inhibited Wnt signaling, and promoted tumor death (Heerma van Voss et al., 2015). In the context of viral infections, a number of studies have suggested the DEAD box proteins DDX1 and DDX3 as promising therapeutic targets for treatment of HIV-1 infection, but such experiments have not yet been completed (Fang et al., 2004; Zhou et al., 2013). In addition to the reported role in influenza SG formation, DDX3 was also implicated in the formation of SGs in HCV infections, which redistribute and co-localize with HCV core protein around lipid droplets to facilitate viral budding. It was shown that silencing of DDX3 and other stress granule components significantly inhibits HCV infection (Pène et al., 2015). Therefore, it is of interest to apply the strategies employed by cancer researchers to the treatment of acute viral infections such as HIV-1, HCV, and VEEV.

In conclusion, our study provides new information regarding host proteins that interact with the functionally uncharacterized VEEV-nsP3. Our data have demonstrated that VEEV-nsP3 associates with DDX1 and DDX3 in infected cells to facilitate viral multiplication. As a putative mechanism for these interactions, we determined that VEEV-nsP3 interacts with a pre-formed translational complex, comprising of DDX3:eIF4A:eIF4G:PABP to potentially aid in translation of viral proteins. Novel components of the nsP3 interactome in infected cells can, therefore, pave the way for novel therapeutic intervention strategies.

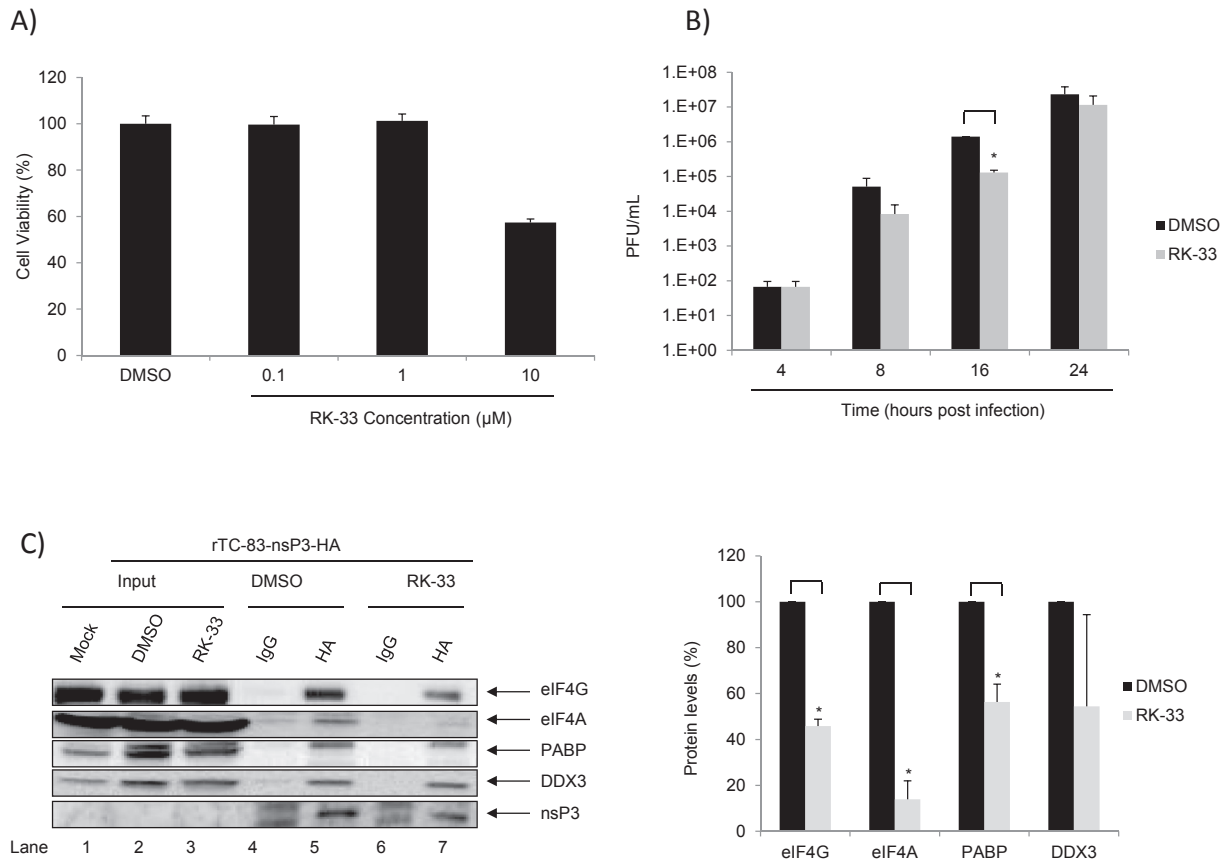


**Fig. 6. RK-33 disrupts VEEV-nsP3 interactions with host translational machinery.** U87MG cells were seeded at 10,000 cells per well in a 96-well plate and treated with varying concentrations of RK-33. At 24 h post treatment cell viability was measured using the Cell Titer Glo Luminescent Cell Viability Assay according to the manufacturer's instructions (A). The graph is representative of 2 independent experiments performed in triplicate and is depicted as a percentage of cell viability. B) U87MG cells seeded in a 96-well plate at a density of 10,000 cells per well were pre-treated with RK-33 for 2 h and infected with rTC-83 (MOI:0.1) for 1 h. Supernatants were collected at 4, 8, 16 and 24 hpi and analyzed by plaque assay. The graph is representative of an independent experiment performed in triplicate. C) U87MG cells were infected with rTC-83-nsP3-HA (MOI:20) for 1 h. At 6 hpi cell lysates were collected, quantified and 2 mg of total protein was immunoprecipitated with an isotype IgG control or an HA antibody. The immunoprecipitates were resolved by SDS-PAGE and the subsequent immunoblot probed with antibodies to eIF4A, eIF4G, PABP, DDX3 or HA. Densitometric counts for eIF4A, eIF4G and DDX3 were obtained using the Quantity One Analysis Software. The normalized data are represented graphically. The western blot is a representative image from 2 independent experiments. \* =  $p \leq 0.05$ .

## Acknowledgments

VEEV pTC83 was a kind gift from Ilya Frolov of the University of Alabama at Birmingham. The following reagents were obtained through the NIH Biodefense and Emerging Infections Research Resources Repository, NIAID, NIH: (i) Venezuelan Equine Encephalitis Virus, TC83 (Subtype IAB), NR63, (ii) Venezuelan equine encephalitis virus Trinidad Donkey (subtype IA/B), NR-332, (iii) Polyclonal Anti-Venezuelan Equine Encephalitis Virus, TC83 (Subtype IA/B) Capsid Protein (antiserum, Goat), NR-9403. We are thankful to Dr. Cynthia de la Fuente with assistance in cloning of rTC-83-nsP3-HA. We are also thankful to Dr. Kyleen Kehn-Hall for providing the VEEV TrD virus.

## Appendix A. Supplementary data

Supplementary data related to this article can be found at <http://dx.doi.org/10.1016/j.antiviral.2016.04.008>.

## References

Akhrymuk, I., Kulemzin, S.V., Frolova, E.I., 2012. Evasion of the innate immune response: the old world alphavirus nsP2 protein induces rapid degradation of Rpb1, a catalytic subunit of RNA polymerase II. *J. Virol.* 86, 7180–7191.

Amaya, M., Keck, F., Lindquist, M., Voss, K., Scavone, L., Kehn-Hall, K., Roberts, B., Bailey, C., Schmaljohn, C., Narayanan, A., 2015. The ubiquitin proteasome system

plays a role in venezuelan equine encephalitis virus infection. *PLoS One* 10, e0124792.

Amaya, M., Voss, K., Sampey, G., Senina, S., de la Fuente, C., Mueller, C., Calvert, V., Kehn-Hall, K., Carpenter, C., Kashanchi, F., Bailey, C., Mogelsvang, S., Petricoin, E., Narayanan, A., 2014. The role of IKK $\beta$  in Venezuelan equine encephalitis virus infection. *PLoS One* 9, e86745.

Anderson, P., Kedersha, N., 2008. Stress granules: the Tao of RNA triage. *Trends Biochem. Sci.* 33, 141–150.

Ariumi, Y., 2014. Multiple functions of DDX3 RNA helicase in gene regulation, tumorigenesis, and viral infection. *Front. Genet.* 5, 423.

Ariumi, Y., Kuroki, M., Abe, K., Dansako, H., Ikeda, M., Wakita, T., Kato, N., 2007. DDX3 DEAD-box RNA helicase is required for hepatitis C virus RNA replication. *J. Virol.* 81, 13922–13926.

Atasheva, S., Fish, A., Fornerod, M., Frolova, E.I., 2010a. Venezuelan equine Encephalitis virus capsid protein forms a tetrameric complex with CRM1 and importin alpha/beta that obstructs nuclear pore complex function. *J. Virol.* 84, 4158–4171.

Atasheva, S., Krendelchikova, V., Liopo, A., Frolova, E., Frolov, I., 2010b. Interplay of acute and persistent infections caused by Venezuelan equine encephalitis virus encoding mutated capsid protein. *J. Virol.* 84, 10004–10015.

Bol, G.M., Vesuna, F., Xie, M., Zeng, J., Aziz, K., Gandhi, N., Levine, A., Irving, A., Korz, D., Tantravedi, S., Heerma van Voss, M.R., Gabrielson, K., Bordt, E.A., Polster, B.M., Cope, L., van der Groep, P., Kondaskar, A., Rudek, M.A., Hosmane, R.S., van der Wall, E., van Diest, P.J., Tran, P.T., Raman, V., 2015. Targeting DDX3 with a small molecule inhibitor for lung cancer therapy. *EMBO Mol. Med.* 7, 648–669.

Buchan, J.R., Parker, R., 2009. Eukaryotic stress granules: the ins and outs of translation. *Mol. Cell* 36, 932–941.

Burgui, I., Aragon, T., Ortin, J., Nieto, A., 2003. PABP1 and eIF4G1 associate with influenza virus NS1 protein in viral mRNA translation initiation complexes. *J. General Virol.* 84, 3263–3274.

Chahar, H.S., Chen, S., Manjunath, N., 2013. P-body components LSM1, GW182,

- DDX3, DDX6 and XRN1 are recruited to WNV replication sites and positively regulate viral replication. *Virology* 436, 1–7.
- Edgcomb, S.P., Carmel, A.B., Naji, S., Ambrus-Aikelin, G., Reyes, J.R., Saphire, A.C., Gerace, L., Williamson, J.R., 2012. DDX1 is an RNA-dependent ATPase involved in HIV-1 Rev function and virus replication. *J. Mol. Biol.* 415, 61–74.
- Fang, J., Kubota, S., Yang, B., Zhou, N., Zhang, H., Godbout, R., Pomerantz, R.J., 2004. A DEAD box protein facilitates HIV-1 replication as a cellular co-factor of Rev. *Virology* 330, 471–480. <http://dx.doi.org/10.1016/j.virol.2004.09.039>.
- Fontaine-Rodriguez, E.C., Taylor, T.J., Olesky, M., Knipe, D.M., 2004. Proteomics of herpes simplex virus infected cell protein 27: association with translation initiation factors. *Virology* 330, 487–492.
- Foy, N.J., Akhrymuk, M., Akhrymuk, I., Atasheva, S., Bopda-Waffo, A., Frolov, I., Frolova, E.I., 2013a. Hypervariable domains of nsP3 proteins of New World and Old World alphaviruses mediate formation of distinct, virus-specific protein complexes. *J. Virol.* 87, 1997–2010.
- Foy, N.J., Akhrymuk, M., Shustov, A.V., Frolova, E.I., Frolov, I., 2013b. Hypervariable domain of nonstructural protein nsP3 of Venezuelan equine encephalitis virus determines cell-specific mode of virus replication. *J. Virol.* 87, 7569–7584.
- Fros, J.J., Domeradzka, N.E., Baggen, J., Geertsema, C., Flipse, J., Vlak, J.M., Pijlman, G.P., 2012. Chikungunya virus nsP3 blocks stress granule assembly by recruitment of G3BP into cytoplasmic foci. *J. Virol.* 86, 10873–10879.
- Fuller-Pace, F.V., 2013. DEAD box RNA helicase functions in cancer. *RNA Biol.* 10, 121–132.
- Galbraith, S.E., Sheahan, B.J., Atkins, G.J., 2006. Deletions in the hypervariable domain of the nsP3 gene attenuate Semliki forest virus virulence. *J. General Virol.* 87, 937–947.
- Garmashova, N., Atasheva, S., Kang, W., Weaver, S.C., Frolova, E., Frolov, I., 2007. Analysis of Venezuelan equine encephalitis virus capsid protein function in the inhibition of cellular transcription. *J. Virol.* 81, 13552–13565.
- Go, Y.Y., Balasuriya, U.B., Lee, C.K., 2014. Zoonotic encephalitis caused by arboviruses: transmission and epidemiology of alphaviruses and flaviviruses. *Clin. Exp. Vaccine Res.* 3, 58–77.
- Heerma van Voss, M.R., Vesuna, F., Trumpi, K., Brilliant, J., Berlinicke, C., de Leng, W., Kranenburg, O., Offerhaus, G.J., Bürger, H., van der Wall, E., van Diest, P.J., Raman, V., 2015. Identification of the DEAD box RNA helicase DDX3 as a therapeutic target in colorectal cancer. *Oncotarget* 6, 28312–28326. <http://dx.doi.org/10.18632/oncotarget.4873>.
- Ishaq, M., Ma, L., Wu, X., Mu, Y., Pan, J., Hu, J., Hu, T., Fu, Q., Guo, D., 2009. The DEAD-box RNA helicase DDX1 interacts with RelA and enhances nuclear factor kappaB-mediated transcription. *J. Cell. Biochem.* 106, 296–305.
- Jose, J., Snyder, J.E., Kuhn, R.J., 2009. A structural and functional perspective of alphavirus replication and assembly. *Future Microbiol.* 4, 837–856.
- Kehn-Hall, K., Narayanan, A., Lundberg, L., Sampey, G., Pinkham, C., Guendel, I., Van Duyne, R., Senina, S., Schultz, K.L., Stavale, E., Aman, M.J., Bailey, C., Kashanchi, F., 2012. Modulation of GSK-3beta activity in Venezuelan equine encephalitis virus infection. *PLoS One* 7, e34761.
- Lai, M.C., Wang, S.W., Cheng, L., Tarn, W.Y., Tsai, S.J., Sun, H.S., 2013. Human DDX3 interacts with the HIV-1 Tat protein to facilitate viral mRNA translation. *PLoS One* 8, e68665.
- Lastarza, M.W., Grakoui, A., Rice, C.M., 1994. Deletion and duplication mutations in the C-terminal nonconserved region of Sindbis virus nsP3: effects on phosphorylation and on virus replication in vertebrate and invertebrate cells. *Virology* 202, 224–232.
- Leung, J.Y., Ng, M.M., Chu, J.J., 2011. Replication of alphaviruses: a review on the entry process of alphaviruses into cells. *Adv. Virol.* 2011, 249640.
- Li, C., Ge, L.L., Li, P.P., Wang, Y., Dai, J.J., Sun, M.X., Huang, L., Shen, Z.Q., Hu, X.C., Ishag, H., Mao, X., 2014. Cellular DDX3 regulates Japanese encephalitis virus replication by interacting with viral un-translated regions. *Virology* 449, 70–81.
- Linerio, F., Welnowska, E., Carrasco, L., Scolaro, L., 2013. Participation of eIF4F complex in Junin virus infection: blockage of eIF4E does not impair virus replication. *Cell. Microbiol.* 15, 1766–1782.
- Lloyd, R.E., 2012. How do viruses interact with stress-associated RNA granules? *PLoS Pathog.* 8, e1002741.
- Malygin, A.A., Bondarenko, E.I., Ivanisenko, V.A., Protopopova, E.V., Karpova, G.G., Loktev, V.B., 2009. C-terminal fragment of human laminin-binding protein contains a receptor domain for Venezuelan equine encephalitis and tick-borne encephalitis viruses. *Biochem. Biokhim.* 74, 1328–1336.
- Narayanan, A., Kehn-Hall, K., Senina, S., Lundberg, L., Van Duyne, R., Guendel, I., Das, R., Baer, A., Bethel, L., Turell, M., Hartman, A.L., Das, B., Bailey, C., Kashanchi, F., 2012. Curcumin inhibits Rift Valley fever virus replication in human cells. *J. Biol. Chem.* 287, 33198–33214.
- Owsianka, A.M., Patel, A.H., 1999. Hepatitis C virus core protein interacts with a human DEAD box protein DDX3. *Virology* 257, 330–340.
- Panas, M.D., Varjak, M., Lulla, A., Eng, K.E., Merits, A., Karlsson Hedestam, G.B., McInerney, G.M., 2012. Sequestration of G3BP coupled with efficient translation inhibits stress granules in Semliki Forest virus infection. *Mol. Biol. Cell* 23, 4701–4712.
- Parker, M.D., Buckley, M.J., Melanson, V.R., Glass, P.J., Norwood, D., Hart, M.K., 2010. Antibody to the E3 glycoprotein protects mice against lethal Venezuelan equine encephalitis virus infection. *J. Virol.* 84, 12683–12690.
- Pène, V., Li, Q., Sodroski, C., Hsu, C.-S., Liang, T.J., 2015. Dynamic interaction of stress granules, DDX3X, and IKK- $\alpha$  mediates multiple functions in hepatitis C virus infection. *J. Virol.* 89, 5462–5477. <http://dx.doi.org/10.1128/JVI.03197-14>.
- Piron, M., Vende, P., Cohen, J., Poncet, D., 1998. Rotavirus RNA-binding protein NSP3 interacts with eIF4G1 and evicts the poly(A) binding protein from eIF4F. *EMBO J.* 17, 5811–5821.
- Scholte, F.E., Tas, A., Albuлесcu, I.C., Zusinaite, E., Merits, A., Snijder, E.J., van Hemert, M.J., 2015. Stress granule components G3BP1 and G3BP2 play a proviral role early in Chikungunya virus replication. *J. Virol.* 89, 4457–4469.
- Shih, J.W., Wang, W.T., Tsai, T.Y., Kuo, C.Y., Li, H.K., Wu Lee, Y.H., 2012. Critical roles of RNA helicase DDX3 and its interactions with eIF4E/PABP1 in stress granule assembly and stress response. *Biochem. J.* 441, 119–129.
- Shin, G., Yost, S.A., Miller, M.T., Elrod, E.J., Grakoui, A., Marcotrigiano, J., 2012. Structural and functional insights into alphavirus polyprotein processing and pathogenesis. *Proc. Natl. Acad. Sci. U. S. A.* 109, 16534–16539.
- Snyder, J.E., Kulcsar, K.A., Schultz, K.L., Riley, C.P., Neary, J.T., Marr, S., Jose, J., Griffin, D.E., Kuhn, R.J., 2013. Functional characterization of the alphavirus TF protein. *J. Virol.* 87, 8511–8523.
- Thulasi Raman, S.N., Liu, G., Pyo, H.M., Cui, Y.C., Xu, F., Ayalew, L.E., Tikoo, S.K., Zhou, Y., April 2016. DDX3 interacts with influenza A NS1 and NP proteins and exerts antiviral function through regulation of stress granule formation. *J. Virol.* 90 (7), 3661–3675.
- Tingting, P., Caiyun, F., Zhigang, Y., Pengyuan, Y., Zhenghong, Y., 2006. Subproteomic analysis of the cellular proteins associated with the 3' untranslated region of the hepatitis C virus genome in human liver cells. *Biochem. Biophys. Res. Commun.* 347, 683–691.
- Valiente-Echeverria, F., Hermoso, M.A., Soto-Rifo, R., Sept 2015. RNA helicase DDX3: at the crossroad of viral replication and antiviral immunity. *Rev. Med. Virol.* 25 (5), 286–299.
- Wang, Y.F., Sawicki, S.G., Sawicki, D.L., 1994. Alphavirus nsP3 functions to form replication complexes transcribing negative-strand RNA. *J. Virol.* 68, 6466–6475.
- Weaver, S.C., Barrett, A.D., 2004. Transmission cycles, host range, evolution and emergence of arboviral disease. *Nat. Rev. Microbiol.* 2, 789–801.
- Wilky, B.A., Kim, C., McCarty, G., Montgomery, E.A., Kammers, K., DeVine, L.R., Cole, R.N., Raman, V., Loeb, D.M., 2015. RNA helicase DDX3: a novel therapeutic target in Ewing sarcoma. *Oncogene*. <http://dx.doi.org/10.1038/ncr.2015.336>.
- Wu, C.H., Chen, P.J., Yeh, S.H., 2014. Nucleocapsid phosphorylation and RNA helicase DDX1 recruitment enables coronavirus transition from discontinuous to continuous transcription. *Cell Host Microbe* 16, 462–472.
- Xu, L., Khadijah, S., Fang, S., Wang, L., Tay, F.P., Liu, D.X., 2010. The cellular RNA helicase DDX1 interacts with coronavirus nonstructural protein 14 and enhances viral replication. *J. Virol.* 84, 8571–8583.
- Yasuda-Inoue, M., Kuroki, M., Ariumi, Y., 2013. DDX3 RNA helicase is required for HIV-1 Tat function. *Biochem. Biophys. Res. Commun.* 441, 607–611.
- Zhou, X., Luo, J., Mills, L., Wu, S., Pan, T., Geng, G., Zhang, J., Luo, H., Liu, C., Zhang, H., 2013. DDX5 facilitates HIV-1 replication as a cellular co-factor of Rev. *PLoS One* 8. <http://dx.doi.org/10.1371/journal.pone.0065040>.